Revised and Updated 2nd Edition

Series Editor
Hisham Abou-Kandil

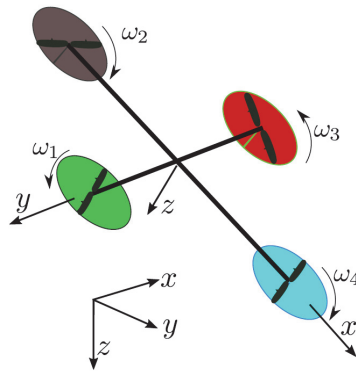# Mobile Robotics

Luc Jaulin

Color section
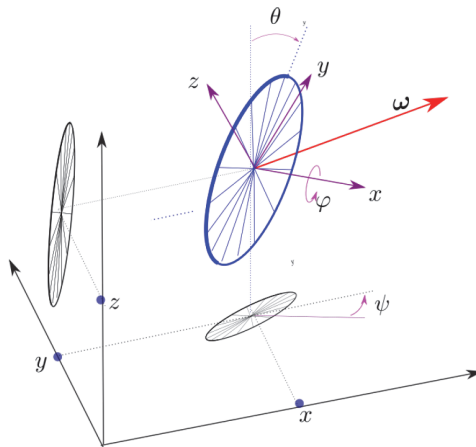
Figure 1.8. Quadrotor

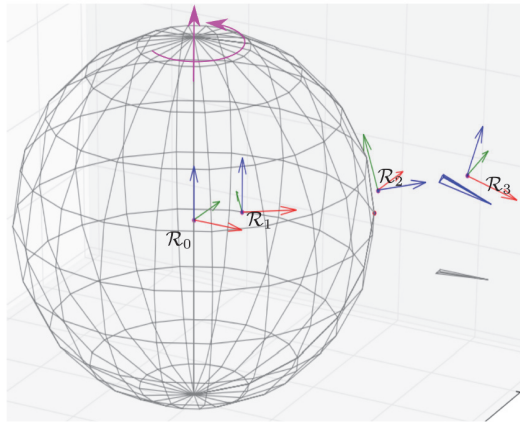

Figure 1.16. Floating wheel

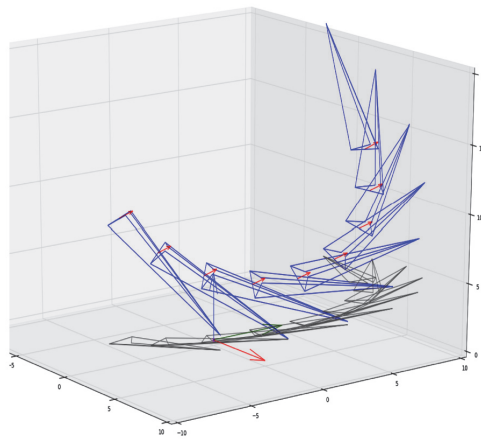**Figure 1.18.** Earth with the different frames. The origin of the frames have been shifted for more visibility
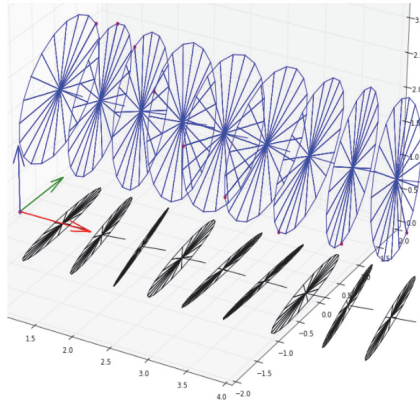

Figure 1.19. Simulation of the underwater robot

Figure 1.21. Motion of the wheel with a torque-free precession

	$\mathbf{p}$			(φ, θ, ψ)			$\mathbf{v_r}$			$\boldsymbol{\omega_r}$		
$\dot{\mathbf{p}}$	0	0	0	0	0	0	1	0	0	0	0	0
	0	0	0	0	0	0	0	1	0	0	0	0
	0	0	0	0	0	0	0	0	1	0	0	0
$(\dot{\varphi}, \dot{\theta}, \dot{\psi})$	0	0	0	0	ω_z	0	0	0	0	1	0	0
	0	0	0	$-\omega_z$	0	0	0	0	0	0	1	0
	0	0	0	ω_y	0	0	0	0	0	0	0	1
$\dot{\mathbf{v_r}}$	0	0	0	0	0	0	0	ω_z	$-\omega_y$	0	0	0
	0	0	0	0	0	0	$-\omega_z$	0	ω_x	0	0	0
	0	0	0	0	0	0	ω_y	$-\omega_x$	0	0	0	0
$\dot{\boldsymbol{\omega}}_r$	0	0	0	0	0	0	0	0	0	0	0	0
	0	0	0	0	0	0	0	0	0	$-\omega_z$	0	$-\omega_x$
	0	0	0	0	0	0	0	0	0	ω_y	ω_x	0

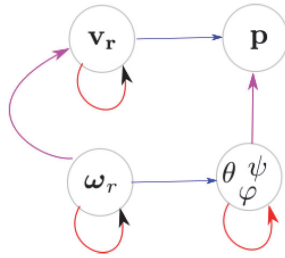**Figure 1.22.** Jacobian matrix of the evolution function at point x₀

Figure 1.23. Graph of the differential delays for the floating wheel
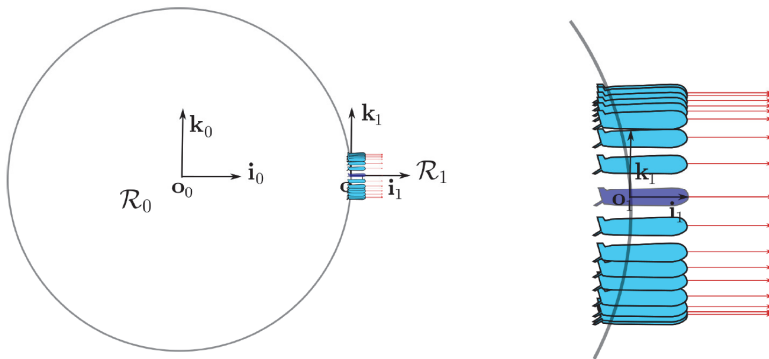

Figure 1.25. Fake periodic trajectory returned by the inertial unit which feels the same as if it were static as for R_1. The corresponding measured acceleration $a_{mes\ r}$ is painted red. The right subpicture corresponds to a zoom around R_1
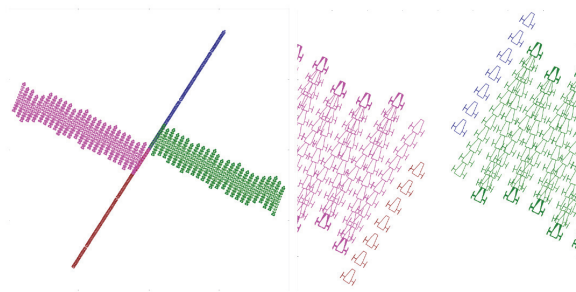
Figure 1.26. Left: simulation of the controller based on the Lie bracket technique. The frame box is [−1, 1] × [−1, 1]. Right: the same picture, but with a frame box equal to [−0.2, 0.2] × [−0.2, 0.2]. To avoid superposition in the picture, the size of the car has been reduced by 1/1000. The length of the forward/backward subpaths corresponds to 10cm approximately
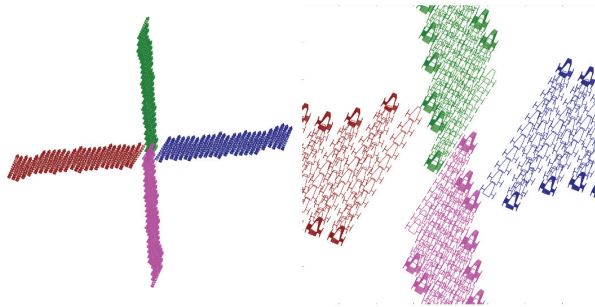

Figure 1.27. Left: The car goes from 0 toward all cardinal directions. The frame box is [−1, 1] × [−1, 1]. Right: the same picture, but with a frame box equal to [−0.2, 0.2] × [−0.2, 0.2]
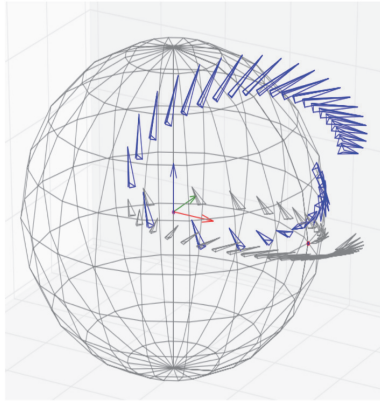
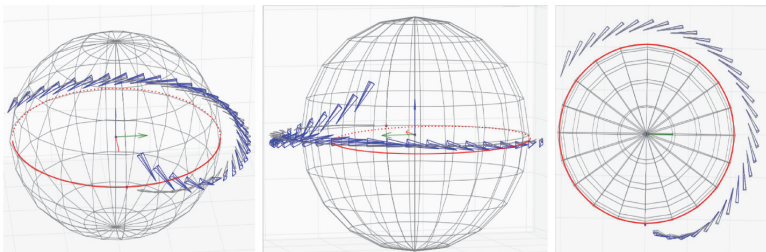**Figure 1.28.** The robot moves like a satellite around the Earth

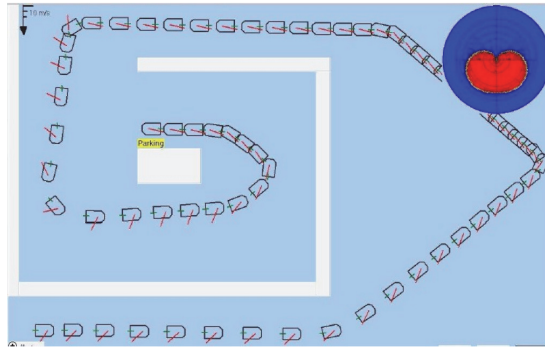**Figure 1.30.** The robot follows the equator toward the east

Figure 2.10. By using a linearizing controller, the robot docks in its place in the harbor; the polar curve is represented on the top right corner
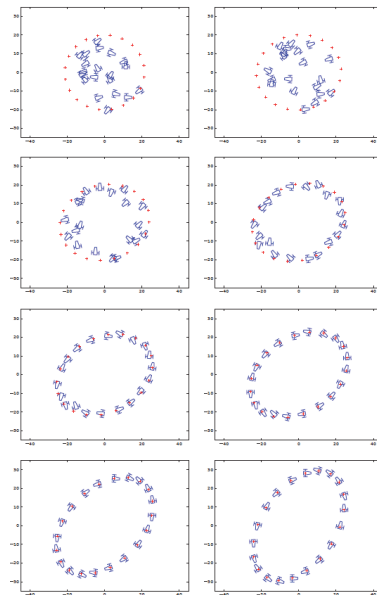

Figure 2.26. During the transient phase, all robots go toward their setpoints in the ellipse. Then, the group exactly follows the deformation of the ellipse
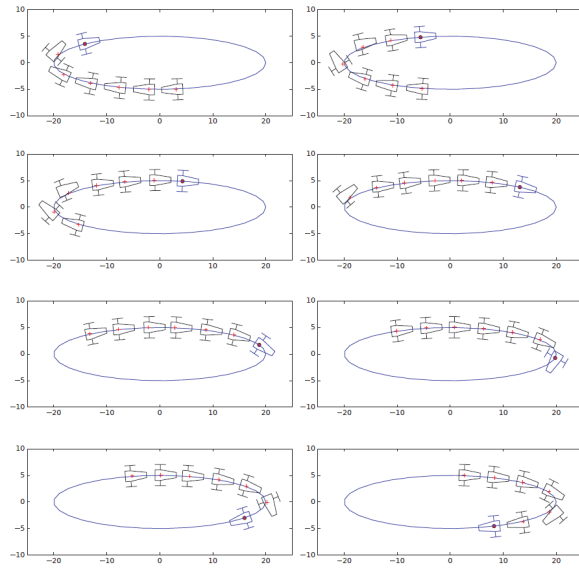
Figure 2.27. After the transient phase, all robots follow the leader with a constant separation distance between two robots
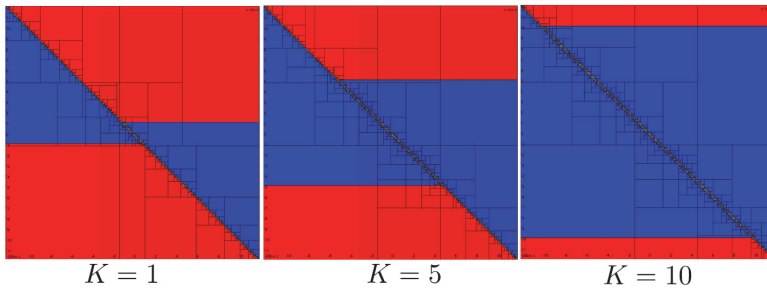

$K = 1$ $K = 5$ $K = 10$

Figure 2.33. Sets S_K for K = 1, 5, 10 in red. When K is large, the probability to go toward the sliding surface increases
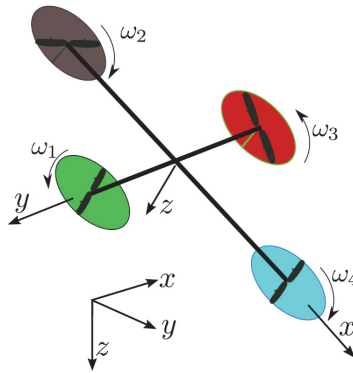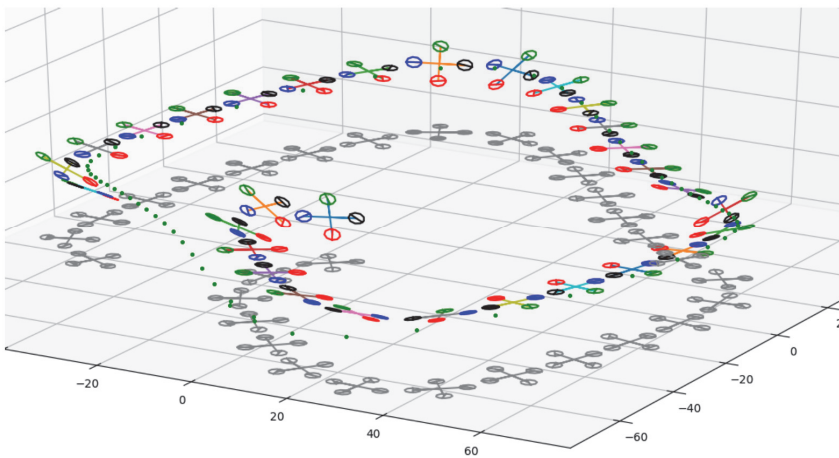
Figure 3.25. The quadrotor to be controlled

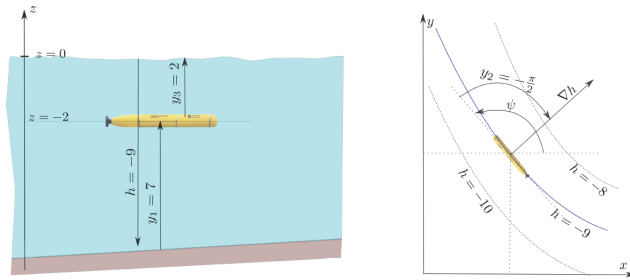**Figure 3.27.** Simulation of the quadrotor which follows the Van der Pol cycle

Figure 3.28. Underwater robot that has to follow an isobath
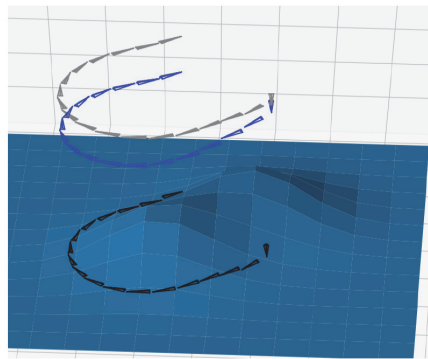

Figure 3.29. Simulation of an underwater robot (blue) following an isobath. The surface shadow (gray) and the seafloor shadow (black) are also depicted. (See exercise 3.8)
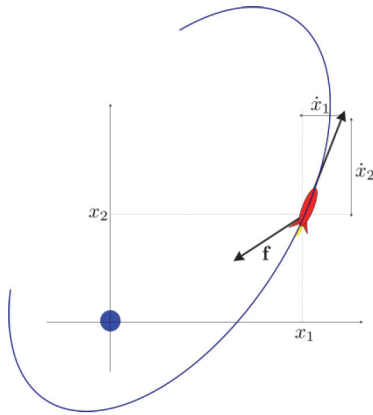
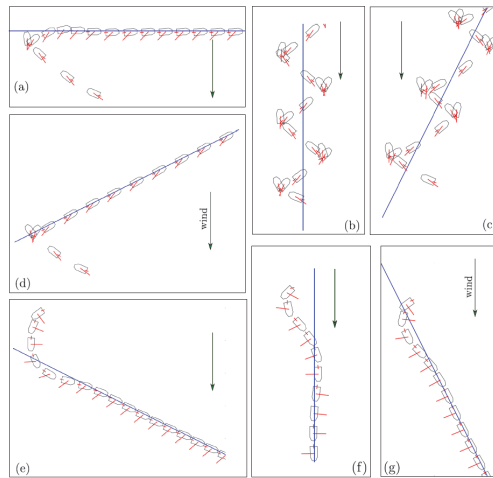**Figure 3.30.** The planet (blue) at coordinates (0, 0) and the satellite (red) at coordinates (x_1, x_2)

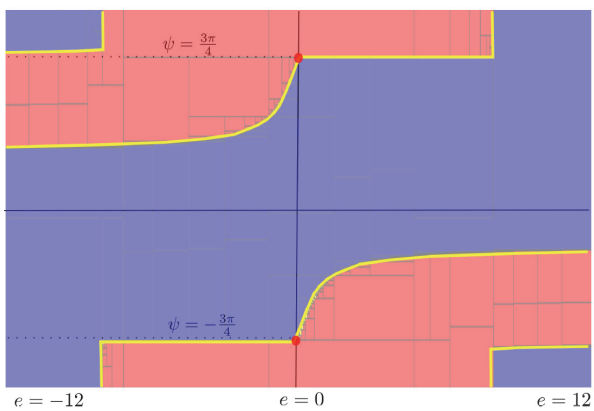**Figure 3.33.** Simulation for the line following of a sailboat
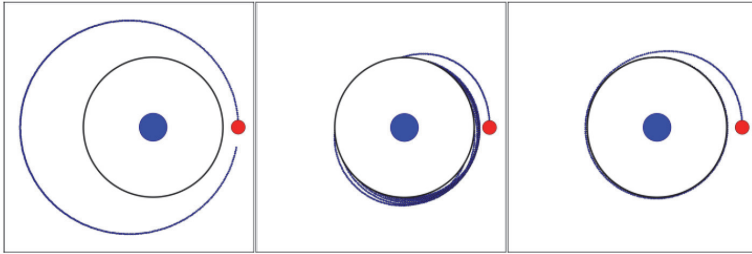
Figure 3.34.

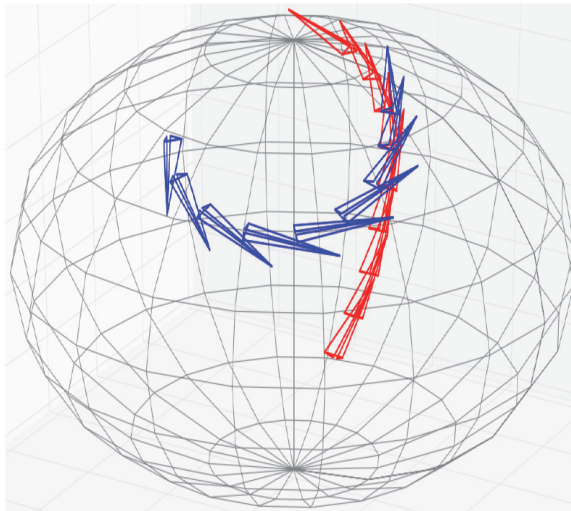**Figure 3.35.**

Figure 3.38.

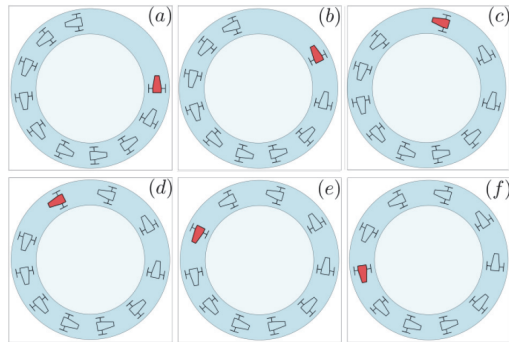**Figure 4.17.** The blue robot R follows the red one R_a

Figure 4.26. (a) initialization at time t = 0; (b)–(f) the controller yields a uniform distribution between cars
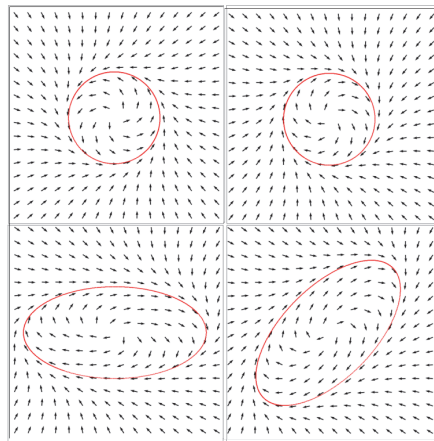

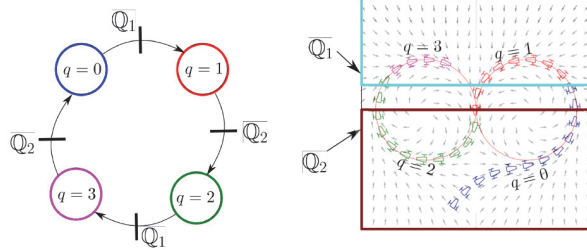**Figure 4.27.** Generation of a vector field with a stable limit cycle corresponding to a specific ellipse

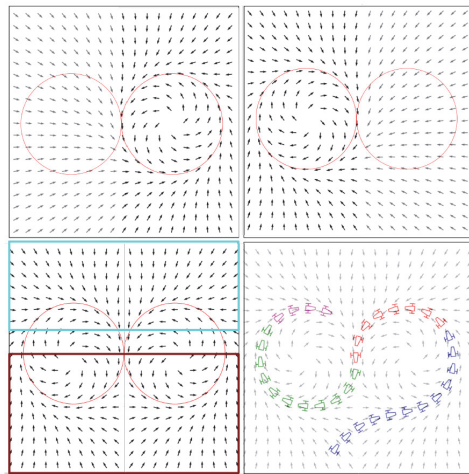**Figure 4.28.** Automaton switching from one field to the other

Figure 4.29. Top: the two vector fields; bottom left: A superposition of the two fields with the two transition sets Q_1, Q_2; Bottom right: the resulting trajectory forms an eight
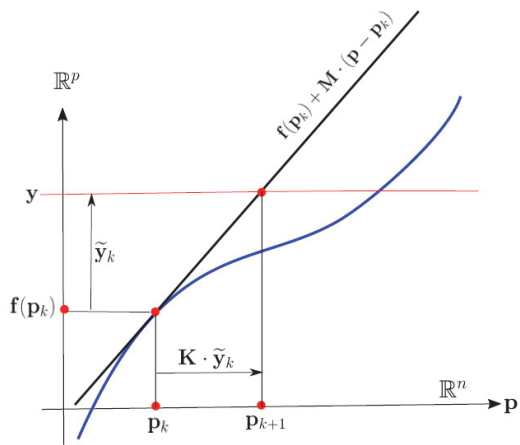
Figure 6.2. The Newton method to minimize $||f(p) - y||_2$